Available online at www.sciencedirect.com
ScienceDirect
Bioorganic & Medicinal Chemistry 16 (2008) 4262–4271
Bioorganic & Medicinal Chemistry

Synthesis, SAR and in vitro evaluation of new cyclic Arg-Gly-Asp pseudopentapeptides containing a *s-cis* peptide bond as integrin $\alpha_v\beta_3$ and $\alpha_v\beta_5$ ligands

Maria Salvati,[a,c] Franca M. Cordero,[a,c,*] Federica Pisaneschi,[a,c] Fabrizio Melani,[b,c,*] Paola Gratteri,[b,c] Nicoletta Cini,[d] Anna Bottoncetti[d] and Alberto Brandi[a,c]

[a]*Department of Organic Chemistry "Ugo Schiff" University of Firenze via della Lastruccia 13, I-50019 Sesto Fiorentino (FI), Italy*
[b]*Department of Pharmaceutical Sciences University of Firenze via U. Schiff 6, I-50019 Sesto Fiorentino (FI), Italy*
[c]*Laboratory of Design, Synthesis and Study of Biologically Active Heterocycles, Polo Scientifico e Tecnologico, University of Firenze, 50019 Sesto Fiorentino (FI), Italy*
[d]*Department of Clinical Physiopathology, Nuclear Medicine Unit University of Firenze viale G. Pieraccini 6, I-50134 Firenze, Italy*

Received 12 November 2007; revised 19 February 2008; accepted 26 February 2008
Available online 29 February 2008

Abstract—The solid-phase synthesis of two diastereomeric cyclic pseudopeptides containing the Arg-Gly-Asp sequence and the dipeptide isostere 2-amino-3-oxotetrahydro-1*H*-pyrrolizine-7a(5*H*)-carboxylic acid (GPTM) is described. Competition binding assays to purified $\alpha_v\beta_3$ and $\alpha_v\beta_5$ integrins with respect to [^{125}I]echistatin showed a high inhibitory activity for the (2*S*,7a*S*)-GPTM derivative. Effects of the structural constraint induced by the two enantiomeric scaffolds (2*R*,7a*R*)-GPTM and (2*S*,7a*S*)-GPTM on the conformation of Arg-Gly-Asp sequence have been computationally investigated using as a reference the recently solved X-ray structure of cyclo(Arg-Gly-Asp-D-Phe-[*N*-Me]Val) in complex with the extracellular fragment of the $\alpha_v\beta_3$ receptor. The computational method disclosed the key role played by a bridging water molecule on differentiating the two ligands by a diverse stabilization of the ligand–protein complex.

1. Introduction

Integrins are a family of cell-surface receptors which mediate cell adhesion processes and, making transmembrane connection to the cytoskeleton, activate many intracellular signalling pathways during morphogenesis, tissue remodelling and repair.[1] These heterodimers are formed by an α and a β subunit non-covalently associated. In particular, in mammals nineteen α subunits and eight β subunits assemble into 24 distinct receptors. Integrins can recognize multiple ligands, generally characterized by the presence of an aspartic acid or a glutamic acid residue, exposed in an extended flexible loop, in a defined recognition sequence. Specificity and efficacy of ligand binding is determined by relative affinity, availability and conformational state of the ligand, together with the integrin subunit composition and its activation state.

Many natural ligands, such as adhesive cell-surface glycoproteins, for example, contain the ubiquitous amino acidic triplet Arg-Gly-Asp.[2] The recognition of the particular conformation of the Arg-Gly-Asp triplet, and of additional binding sites, assures a high substrate specificity among the different integrins that bind this common sequence.

Among the Arg-Gly-Asp-dependent integrins, the $\alpha_v\beta_3$[3] and $\alpha_v\beta_5$[4] receptors have received increasing attention as therapeutic targets as they are expressed in various cell types such as endothelial cells, platelets, osteoclasts, mel-

Abbreviations: All, allyl; DIC, *N*,*N*′-diisopropylcarbodiimide; DIPEA, *N*,*N*-diisopropylethylamine; DMAP, 4-dimethylaminopyridine; DMF, *N*,*N*-dimethylformamide; Fmoc, 9H-fluoren-9-yl-methyloxycarbonyl; HOBt, 1-hydroxybenzotriazole; NMM, *N*-methylmorpholine; Pbf, 2,-2,4,6,7-pentamethyl-2,3-dihydrobenzofuran-5-sulfonyl; TBTU, 2-(1*H*-benzotriazol-1-yl)-1,1,3,3-tetramethyluronium tetrafluoroborate; TFA, trifluoroacetic acid.

Keywords: Hydrogen bonds; Molecular dynamics; Nitrogen heterocycles; RGD.

* Corresponding authors. Tel.: +39 055 457 3498; fax: +39 055 457 3531 (F.M.C.); tel.: +39 055 457 3703; fax: +39 055 457 3671 (F.M.); e-mail addresses: franca.cordero@unifi.it; fabrizio.melani@unifi.it

0968-0896/$ - see front matter © 2008 Elsevier Ltd. All rights reserved.
doi:10.1016/j.bmc.2008.02.080

anoma and smooth muscle cells. They are, therefore, involved in processes as diverse as osteoporosis, arthritis, retinopathy, tumour-induced angiogenesis and metastasis formation. $\alpha_v\beta_3$ Antagonists, including Arg-Gly-Asp-containing peptides, have been successfully used to inhibit blood vessel development and tumour growth in different models.[5] Moreover, it has been demonstrated that $\alpha_v\beta_3$ integrin is also involved in other processes that characterize tumour growth and metastasis. For example, its expression is up-regulated on metastatic melanoma[6] and late stage glioblastoma.[7] Recent studies have also implicated the $\alpha_v\beta_5$ integrin in angiogenesis, possibly through a distinct signalling pathway, activated by different growth factors.[4c]

In the past decade the first generation cyclic peptide cyclo(Arg-Gly-Asp-D-Phe-Val) (**1**), selective for the $\alpha_v\beta_3$ integrin, was developed by Kessler and co-workers by means of the 'spatial screening' procedure (Fig. 1).[8] In particular, the structure–activity relationship (SAR) study performed on a library of diastereomeric cyclic peptides cyclo(Arg^{I}-Gly^{II}-Asp^{III}-Xxx^{IV}-Yyy^{V}),[8] enabled to determine the influence of residues at positions IV and V on the $\alpha_v\beta_3$ inhibition. It was found, for example, that high inhibition activity was assured by the presence in IV of an aromatic, hydrophobic D-amino acid (or, alternatively, a D-serine), or of a glycine.

On the contrary, the substitution pattern at position V did not have a great influence on the $\alpha_v\beta_3$ inhibition, but a somewhat lower activity was in general found when the D-amino acid occupied this position of the cyclopeptide sequence.

Accordingly, many different cyclic Arg-Gly-Asp-containing peptides have been synthesized by the replacement of the central D-Phe-Val residue with different turn mimetics and sugar amino acids, with the aim of increasing the conformational constraint of the Arg-Gly-Asp sequence.[9] In particular, the N-methylated derivative cyclo(Arg-Gly-Asp-D-Phe-[*N*-Me]Val) (cilengitide, EMD121974, **2**) is being investigated in clinical phase II as an angiogenesis inhibitor.[9b,10] More recently, also non-peptidic antagonists, both linear and cyclic, have been studied, because of their enhanced metabolic stability, bioavailability and biological absorption.[4a,11] However, peptidomimetic compounds are still of great therapeutic interest due to their higher proteolytic stability, compared to the peptidic analogues.

Recently, we reported the design and the synthesis of novel bicyclic lactams which are mimetics of conformationally constrained Gly-(*s-cis*)-Pro dipeptides (GPTMs)

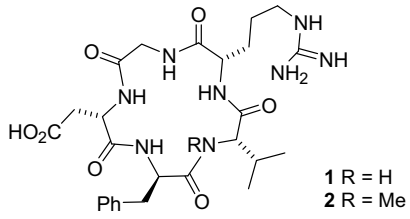

Figure 1. Kessler's integrin ligands.

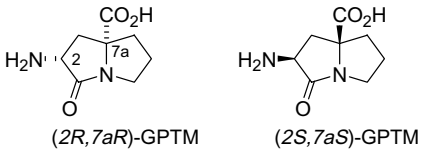

Figure 2. Bicyclic mimetics of Gly-(*s-cis*)-Pro dipeptides.

(Fig. 2).[12,13] Theoretical and experimental conformational analysis on model peptides demonstrated that these scaffolds are able to mimic the central dipeptide of a type VI β-turn.[12d,e] Therefore, it was interesting to evaluate GPTMs as dipeptide isosteres to replace the D-Phe-[*N*-Me]Val unit in Kessler's lead compound **2** and to evaluate the integrin affinity of the new modified cyclic peptides.

Then, the solid-phase synthesis of the cyclic pseudopentapeptide cyclo[Arg-Gly-Asp-GPTM] and its in vitro biological evaluation in competition binding assays to purified $\alpha_v\beta_3$and $\alpha_v\beta_5$ with respect to [^{125}I]echistatin was carried out.[14] The different affinity of the new diastereomeric ligands containing (2*R*,7a*R*)-GPTM and (2*S*,7a*S*)-GPTM suggested a molecular dynamic simulation of the binding site of integrin $\alpha_v\beta_3$ complexed with synthesized ligands in comparison with ligands **1** and **2**, which offered an insight to justify the different affinity of pseudopentapeptides cyclo[Arg-Gly-Asp-GPTM].

2. Results and discussion

The synthesis of cyclo[Arg-Gly-Asp-(2*R*,7a*R*)-GPTM] (**5**) and cyclo[Arg-Gly-Asp-(2*S*,7a*S*)-GPTM] (**6**) was efficiently carried out using the well-established strategy of the head-to-tail cyclization of a peptide anchored to the resin through the side chain of a trifunctional amino acid,[15] in this case the aspartic acid side chain.[16]

Following this approach, the linear target peptides **4** were synthesized starting from aspartic acid linked to Wang resin **3** through its side chain and using the Fmoc/*t*-Bu/OAll protection strategy. Fmoc-Asp-OAll was anchored to the Wang resin using the DIC/DMAP coupling system with an average loading of the resin 0.25–0.35 mmol/g. Successive coupling of *N*-Fmoc-Gly-OH and *N*-Fmoc-Arg(Pbf)-OH was achieved by using 3 equivalents of the amino acids and a mixture of HOBt (3 equiv), TBTU (3 equiv) and NMM (6 equiv). The bicyclic amino acids (2*R*,7a*R*)-*N*-Fmoc-GPTM-OH and (2*S*,7a*S*)-*N*-Fmoc-GPTM-OH[12] underwent coupling under the same conditions with complete conversion using only 1.2–1.5 equivalents, to give the linear peptide **4** (Scheme 1).

Deprotection of the C- and N-terminal residues caused the smoothly cyclization in the presence of TBTU and DIPEA. Further treatment of the resin with TFA released the **5** and **6** cyclic peptides completely deprotected at the side chains.

A drawback of our strategy was the obtainment of very polar peptides, but it could be overcome by an initial purification of the crude mixtures by flash chromatography

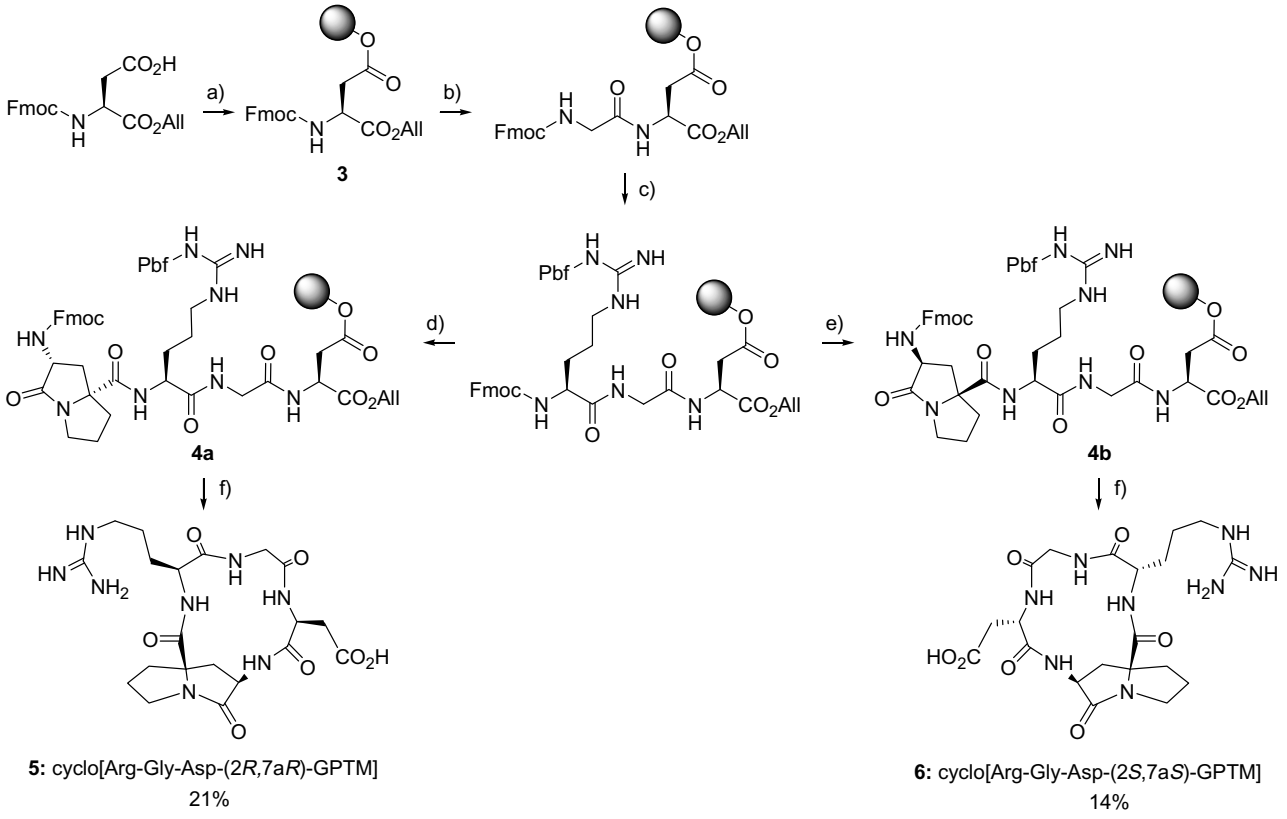

Scheme 1. Solid-phase synthesis of cyclo(Arg-Gly-Asp-GPTM) peptides. Reagents and conditions: (a) i—DIC, DMAP, Wang resin; ii—Ac_2O, NMM; (b) i—piperidine/DMF 20%; ii—Fmoc-Gly-OH, HOBt, TBTU, NMM; (c) i—piperidine/DMF 20%; ii—Fmoc-Arg(Pbf)-OH, HOBt, TBTU, NMM; (d) i—piperidine/DMF 20%; ii—Fmoc-(2*R*,7a*R*)-GPTM-OH, HOBt, TBTU, NMM; (e) i—piperidine/DMF 20%; ii—Fmoc-(2*S*,7a*S*)-GPTM-OH, HOBt, TBTU, NMM; (f) i—$PhSiH_3$, $Pd(PPh_3)_4$; ii—piperidine/DMF 20%; iii—TBTU, DIPEA; iv—TFA.

on silica gel [eluent: CH_2Cl_2/MeOH (1% TFA) 10:1 → 2:1] followed by a RP HPLC on a highly polar Hypercarb 100 × 10 mm (7 μm) column, which gave pure compounds **5** and **6** in 21% and 14% overall yield with respect to *N*-Fmoc-Asp(Wang resin)-OAll loading, respectively.

In vitro test of ability of the cyclic pentapeptides **5** and **6** to compete with [^{125}I]echistatin[17,18] in binding with $\alpha_v\beta_3$ and $\alpha_v\beta_5$ integrins were carried out (see Section 5). In particular, integrin-coated 96-well plates were incubated with the radiolabelled ligand in the presence of serially diluted competing compounds **5** and **6** and radioactivity was measured with a γ-counter. Relative affinity values (IC_{50}) were determined by fitting binding inhibition values by non-linear regression (Table 1).

Low activity was observed with peptide **5**, whereas its diastereomer **6** showed high inhibition values for the binding of both $\alpha_v\beta_3$ and $\alpha_v\beta_5$ (Table 1). Interestingly, the comparison with affinity of reference compounds **1** and **2**, shows that **6** displayed a similar activity against both the receptors, and higher, or comparable, for $\alpha_V\beta_3$ integrin compared to **1** and **2**. On the other hand, the affinity of **6** for $\alpha_V\beta_5$ was 100 times lower compared to both Kessler's peptides.

Cyclopeptide **6**, therefore, is an effective ligand of $\alpha_V\beta_5$ and $\alpha_V\beta_3$ integrins.

Table 1. Inhibition of [^{125}I]echistatin binding to $\alpha_v\beta_5$ and $\alpha_v\beta_3$ for peptides **5**–**6**

Ligand	$\alpha_v\beta_5$ IC_{50} (nM)	$\alpha_v\beta_3$ IC_{50} (nM)
5	7960 ± 790[a]	2150 ± 1400[a]
6	14.3 ± 1.4[a]	34.4 ± 9.8[a]
1	0.11[9g]	196[9g]
2	0.13[9g]	18.9[9g]

Values are the mean of three-independent determinations. The corresponding values previously determined for Kessler's ligands **1** and **2** (see Ref. 9g) were reported for comparison.

[a] Values represent means ± SEM of two-independent experiments, each performed in triplicate.

It should be mentioned at this point that, compared to the compounds analysed by Kessler, peptides **5** and **6** present a significant difference. Kessler's cyclic ligands **1** and **2** are *all-trans* peptides, whereas peptides **5** and **6** contain the conformationally restricted Gly-(*s-cis*)-Pro mimetic GPTM at positions IV and V. In particular, peptide **5** has an α-substituted (*s-cis*)-L-proline[19] at position V and **6** presents the corresponding (*s-cis*)-D-proline[19] at the same position.

The affinity data proved that the introduction of the Gly-(*s-cis*)-Pro mimetic (2*S*,7a*S*)-GPTM in the cyclic peptide does not destroy its affinity for integrins, and induce important variations in the Arg-Gly-Asp confor-

mation with respect to the analogues *all-trans* peptides. Interestingly, in this case, in contrast to Kessler's observation, the presence at position V of the peptide of a D-amino acid mimetic (a formal D-(*R*)-proline)[19] significantly increases the integrin affinity, compared to isomer **5** which experiences a mimetic L-residue at the position V and a D-amino acid at the IV position (see above).

The observed different activity of cyclopeptides **5** and **6** prompted us to undertake a structural study aiming to get a general insight of the factors influencing the affinity towards integrins and hints for the design of new ligands.

Recently, the X-ray structure of Kessler's peptide **2** in complex with the extracellular fragment of the $\alpha_v\beta_3$ receptor (Protein Data Bank, entry 1L5G) has been reported.[20] According to the X-ray data, ligand **2** bound to the $\alpha_v\beta_3$ integrin is characterized by an extended conformation of the Arg-Gly-Asp sequence with an 8.9 Å distance between C_β Asp and C_β Arg. The Asp residue occupies the $(i+1)$ position of an inverse γ-turn and the $(i+2)$ position of a distorted βII′-turn. The Arg and Asp side chains point opposite directions. The guanidinium group of the Arg is involved in a salt bridge with Asp^{218} and Asp^{150}. At the opposite side Asp contacts the metal ion in the metal ion-dependent adhesion site (MIDAS) with one of its carboxylate oxygens and makes a hydrogen bond with Asn^{215}.

The crystal structure of this protein/ligand complex provides a general model for the interaction of integrins with their antagonists. In fact, docking studies and molecular dynamic simulations based on this model, and performed on several peptidic and non-peptidic ligands,[9f,g,21] corroborated the general ligand structural requirements and the presence of the above mentioned main ligand–receptor interactions.

In order to rationalize the observed differences of diastereomers **5** and **6** in bioactivity, the conformations assumed by the Arg-Gly-Asp adhesive motif embedded in the *cyclo*-pentapeptides were analyzed by a MD simulation. In particular, either the free ligands **1**, **2**, **5** and **6** in H_2O and the corresponding $\alpha_v\beta_3$ integrin/ligand/H_2O complexes were studied.

The simulation of ligands in water was performed taking into account a 10 Å layer of water molecules around the ligand. The structures of complexes **B**, **C**, **D** between $\alpha_v\beta_3$ integrin and ligands **6**, **1** and **5**, respectively, were built using the crystal structure of the **2**/$\alpha_v\beta_3$ complex **A** as a model. Some restrictions were imposed during the MD simulation of the four complexes **A**–**D** in water (see Section 5). Two 0.5 ns runs were performed for each complex **A**–**D** and one 0.5 ns simulation for ligands **1**, **2**, **5** and **6** in water at 310 K, sampling one conformation every 0.5 ps. The collected conformations were then used for the structural study.

Several geometrical parameters including the average distances between atoms common to the four ligands (see Fig. 3) and the *Ψ* and *Φ* dihedral angles of Arg, Gly and Asp were calculated for all the conformations collected during the MD and compared in the free ligands and in the complexes.

The MD simulations of the free ligands in water were not indicative as the means of Arg-Gly-Asp geometrical data were statistically the same ($F < 1$).[22] In particular, the conformational freedom of all ligands was highly sufficient to allow the Arg-Gly-Asp amino acid residues to assume similar spatial arrangements, either in active or in non-active peptides. This fact ruled out the possibility of NMR conformational studies on ligands **5** and **6** in water, to understand the different bioactivity of the two diastereomers.[23] On the contrary, important information was achieved from the study of the complexes.

As expected, the protein–ligand interaction resulted in a decrease in entropy associated with a loss of conformational freedom within the ligand and specifically within the Arg-Gly-Asp moiety. The average values of the calculated dihedral angles and distances of the active ligand **6** in complex **B** were consistent with the corresponding values of the reference compound **2**. The inactive analogue **5** gave values clearly in disagreement with **2**. The most significant values are reported in Tables 2 and 3.

Statistically significant ($F > 1$) variations in the relative spatial arrangement of atoms and groups, able to interact with the protein through hydrogen bonds and salt bridge, were found between the active ligands **1**, **2**, **6** and the inactive derivative **5**. Indeed, the major differences involved the trigonal carbon atoms in Arg and Asp side chains (C_I and C_{III}), the Gly and Arg nitrogen and carboxylic oxygen atoms (N_{II}, O_{II}, N_{III} and O_{III}) and the nitrogen atom of the fourth residue (N_{IV}) (Fig. 3 and Table 3). The main difference was the shortest N_{II}–C_{III} distance found in complex **D**.

In spite of the variations in geometrical parameters, calculations showed the same main interactions between the residues of ligands **1**, **2**, **5** and **6** and the integrin receptor. In agreement with the reference crystal structure,[20] the Asp residue was found to interact through its carboxylate group with a Mn^{2+} ion and the backbone amide of Asn^{215} and Tyr^{122}, while Arg contacted the Asp^{150} and Asp^{218}. Accordingly, all these interactions appear to be necessary for the molecular recognition of the Arg-Gly-Asp ligands but cannot serve as a criterion for determining their differences in affinity.

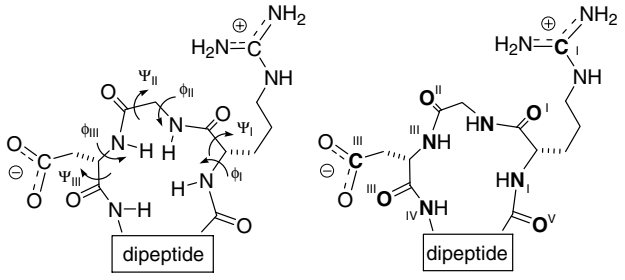

Figure 3. Dihedral angle and atomic numbering schemes of the Arg-Gly-Asp ligands.

Table 2. Average dihedral angle values (degree) calculated for complexes **A**–**D** in the MD simulations

Ligand/ complex (run)		Angles (standard deviation)					
		ϕ_I	ψ_I	ϕ_{II}	ψ_{II}	ϕ_{III}	ψ_{III}
5/D	(1)	−71.7 (21.9)	114.7 (13.4)	80.5 (15.8)	−91.7 (23.6)	−118.4 (20.5)	72.1 (16.4)
	(2)	−69.2 (18.8)	102.0 (23.0)	101.3 (25.7)	−89.3 (22.9)	−124.3 (18.2)	61.9 (14.9)
6/B	(1)	−82.4 (13.1)	135.4 (12.1)	71.2 (13.7)	−126.4 (13.4)	−93.1 (15.0)	95.5 (10.3)
	(2)	−83.0 (14.8)	141.1 (10.5)	69.4 (10.4)	−125.7 (18.7)	−102.6 (22.8)	87.6 (13.3)
1/C	(1)	−118.4 (13.3)	144.3 (13.8)	65.6 (11.9)	−149.0 (10.8)	−71.6 (10.4)	85.8 (10.8)
	(2)	−112.8 (15.3)	142.8 (13.9)	64.6 (11.5)	−149.9 (11.8)	−73.5 (11.8)	89.1 (13.7)
2/A	(1)	−98.7 (16.8)	133.6 (22.0)	74.1 (19.6)	−145.4 (15.1)	−77.1 (16.1)	92.2 (13.8)
	(2)	−98.8 (16.8)	133.0 (21.2)	76.7 (2.7)	−145.1 (18.5)	−79.7 (19.6)	91.7 (12.6)

For the angle numbering see Figure 3.

Table 3. Average distances (Å) between selected atoms of complexes **A**–**D** as found in MD simulations and variance ratio *F*

Ligand/ complex (run)		Average distances (Å)							
		C_I–O_{II}	N_{II}–C_{III}	N_{II}–O_{II}	O_{II}–C_{III}	O_{II}–O_{III}	O_{II}–N_{IV}	N_{III}–C_{III}	C_{III}–N_{IV}
5/D	(1)	10.4	6.1	3.2	3.7	5.1	4.0	3.1	4.9
	(2)	10.6	6.2	3.2	3.6	5.1	4.2	3.2	4.9
6/B	(1)	9.3	7.3	2.9	5.1	4.6	3.6	3.8	4.2
	(2)	8.8	7.1	2.9	4.7	4.8	3.7	3.7	4.3
1/C	(1)	9.4	7.4	2.8	5.3	4.3	3.0	3.8	4.3
	(2)	9.4	7.4	2.8	5.2	4.3	3.1	3.8	4.3
2/A	(1)	9.7	7.4	2.9	5.2	4.3	3.2	3.8	4.4
	(2)	9.7	7.3	2.9	5.2	4.4	3.3	3.8	4.4
	F	1.97	7.12	1.17	5.07	1.46	1.04	5.57	2.34

For the atom numbering see Figure 3.

From the MD simulations appeared that the Gly residue probably plays a key role in the inhibition activity. Actually, Zhang and co-workers[20] evinced that this amino acid makes several hydrophobic interactions with the α subunit of the protein, but is not involved in any direct hydrogen bonding with the protein residues, being far away from suitable donor or acceptor atoms. Additional contacts through water molecules were not established but not excluded.

The analysis of complexes **B** and **D** showed a striking difference regarding the presence of a water molecule between the NH of the Gly residue of **6** and the carboxylate group of Asp^{218} (Fig. 4, **B**). This molecule was not present in complex **D** (Fig. 4, **D**). The distortion of the backbone geometry of **5**, in fact, causes an orientation of the NH group of Gly unsuitable to coordinate the water molecule in a rigid network of hydrogen bonds. Interestingly, the dynamic simulation of complexes **A** and **C**, with Kessler's active ligands **1** and **2**, showed the presence of the same bridging water molecule between the Gly residue and Asp^{218} (Fig. 5).

The strength of the intramolecular $N_{IV}H\ldots O_{II}$ hydrogen bond in complexed ligands seems to be a key factor to determine the most effective conformation of the Gly residue in the ligands. In the cyclic ligands **5** and **6** the N_{IV} donor–O_{II} acceptor distance varies from 4.1 to 3.6 Å, respectively (Fig. 4). This distance ranges between 3.1 and 3.2 Å in complexed ligands **1** and **2** (Fig. 5), much closer to the value for the active ligand **5**.

Therefore, the Gly–Asp^{218} interaction mediated by the bridging water molecule appears to be the key element to assure the most effective interaction of the ligand with the $\alpha_V\beta_3$ receptor. This observation seems to better accommodate the role of Gly in the interaction with the receptor assigned by the authors of the crystal structure only to hydrophobic interactions.[20] It is worth to be noted that this bridging water, and this interaction, consequently, could not be resolved in the reference crystal structure. To our knowledge, this is the first time this observation is made in computational studies on Arg-Gly-Asp ligand/$\alpha_v\beta_3$ interaction.

3. Conclusion

Two novel Arg-Gly-Asp-containing cyclic peptides **5** and **6**, incorporating a conformationally restricted Gly-(*s-cis*)-Pro mimetic GPTM, were synthesized by means of solid-phase peptide synthesis. They were tested in vitro for their ability to compete with the [^{125}I]echistatin ligand for the binding to $\alpha_V\beta_3$and $\alpha_V\beta_5$ receptors and compared with the lead compounds of this class of antagonists, **1** and **2**. The (2*S*,7a*S*)-GPTM derivative **6** showed high inhibitory activity against both receptors, comparable with that of the two reference compounds. A structural study performed by MD simulation and based on the X-ray structure of the **2**/$\alpha_v\beta_3$ complex allowed to determine the main interactions required for the ligand–receptor recognition, which proved to be in agreement with the model X-ray structure. Moreover,

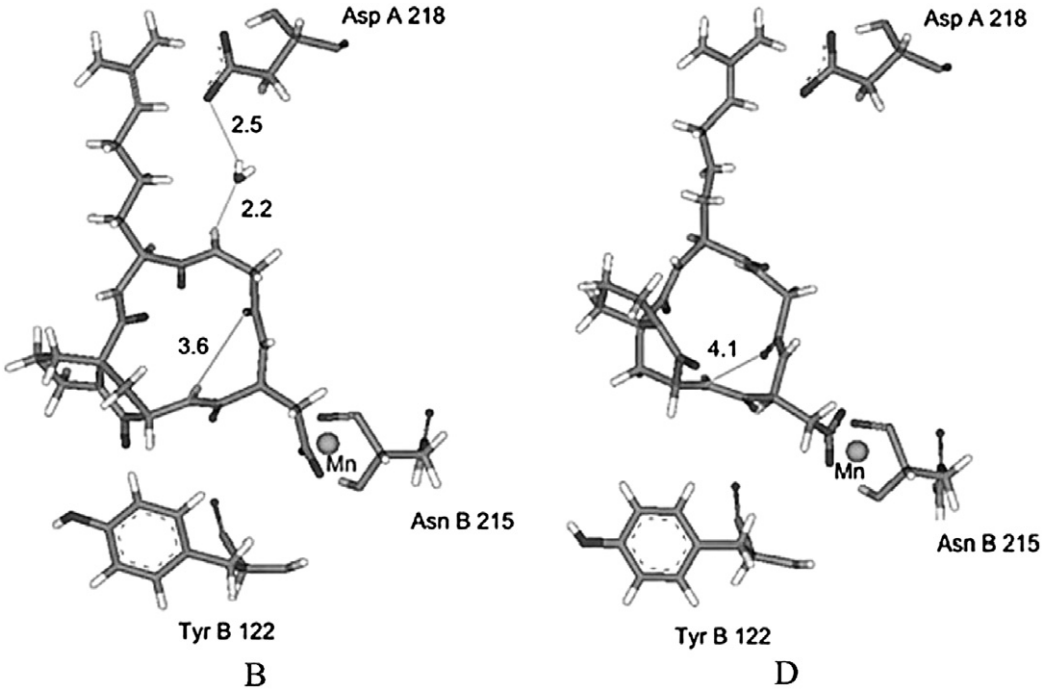

Figure 4. Calculated mean structures of ligands **6** (**B**) and **5** (**D**) in complexes **B** and **D**. Only the bridging water molecule and some residues of the active site are shown for clarity. Selected hydrogen bonds are reported.

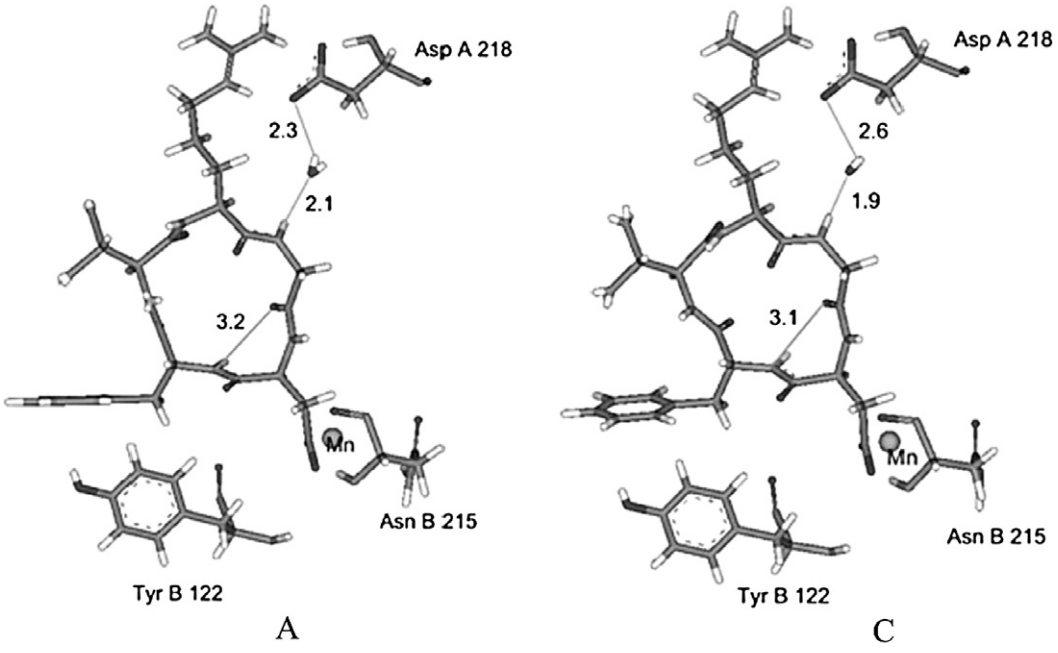

Figure 5. Calculated mean structures of ligands **2** (**A**) and **1** (**C**) in complexes **A** and **C**. Only the bridging water molecule and some residues of the active site are shown for clarity. Selected hydrogen bonds are reported.

the collected data suggested that the difference in affinity of ligands **5** and **6** could be rationalized by the involvement of a bridging water molecule in the ligand-$\alpha_v\beta_3$ receptor interaction between the NH of Gly in the ligand and the carboxylate group of Asp^{218} in the receptor. The contribution of the water molecule was critical for the stabilization of the complex also for active ligands **1** and **2**. Therefore, variations in conformation of the Arg-Gly-Asp triplet induced by the enantiomeric dipeptide isosteres GPTMs affected the ligand activity of **5** and **6** modifying their ability in fixing the water molecule in the active site.

This new observation represents an extremely useful method and criterion to the rational design of novel integrin antagonists.

4. Computational methods

4.1. Ligand and complex setup

Ligand structures were generated from the standard fragment library of the BUILDER module of the INSIGHT II program (software version 2005)[24] according to the X-ray data of the ligand **2** bound to the $\alpha_v\beta_3$ integrin. Geometry optimizations were achieved with the CFF91 force field of DISCOVER module of the INSIGHT II program by applying the Conjugate Gradients algorithm with a convergence criterion of 0.01 kcal/mol.

4.2. Molecular dynamic simulation

To assess the preferred conformations of ligands bound to the $\alpha_v\beta_3$ integrin, two 0.5 ns molecular dynamic (MD) simulations of the complex were carried out. The following restrictions were imposed during the MD simulation of the four complexes **A**–**D** in water: (a) only the receptor amino acidic residues within a radius of 15 Å from the centre of the binding site were considered; (b) the protein backbone was required to be rigid, whereas torsional flexibility of its side chains was allowed; (c) only a layer of 10 Å of water around the ligands was considered; (d) the Mn^{2+} ions present in the X-ray solved structure were replaced by Ca^{2+} ions, because of the lack of parameters for Mn^{2+} ions in the used program.

Calculations were carried out with the DISCOVER module of the INSIGHTII program using CFF91 force field. A multiple-step procedure was used. The complex was energetically minimized using the Conjugate Gradients algorithm until the derivative of the potential energy was less than 0.01 kcal/mol.

The minimized solvated system was used as initial structure for the subsequent MD simulation. The system was heated gradually to 310 K. Coordinates were saved every 0.5 ps yielding 1000 structures. Minimization and dynamic simulation were carried out keeping the backbone atoms of the selected $\alpha_v\beta_3$ integrin portion constrained.

5. Experimental

5.1. Solid-phase receptor binding assay

[^{125}I]Echistatin, labelled by the lactoperoxidase method to a specific activity of 2000 Ci/mmol, was purchased from Amersham Pharmacia Biotech. Integrins $\alpha_V\beta_3$ (0.35 mg/mL, 25 μg in 71.4 μL) and $\alpha_V\beta_5$ (1.035 mg/mL, 25 μg in 24.1 μL) purified from human placenta were purchased from CHEMICON International Inc., Temecula, CA. The receptor binding assay was performed as described by Kumar et al.[17] Purified receptors $\alpha_V\beta_3$ and $\alpha_V\beta_5$ were diluted, respectively, at 500 ng/mL and 1000 ng/mL in coating buffer [20 mM Tris (pH 7.4), 150 mM NaCl, 2 mM $CaCl_2$, 1 mM $MgCl_2$, 1 mM $MnCl_2$]. An aliquot of the diluted receptors (100 μL/well) was added to a 96-well microtiter plate and incubated overnight at 4 °C. The coating solution was removed and 200 μL of blocking/binding buffer [50 mM Tris–HCl (pH 7.4), 100 mM NaCl, 2 mM $CaCl_2$, 1 mM $MgCl_2$, 1 mM $MnCl_2$, 1% bovine serum albumin] was added to the wells, which were incubated an additional 2 h at room temperature. The plate was rinsed twice with the same buffer and incubated for 3 h at room temperature with radiolabelled ligand at variable concentrations (0.02–5.0 nM) to determine saturation binding isotherms of [^{125}I]echistatin to $\alpha_V\beta_3$ and $\alpha_V\beta_5$, respectively. Non-specific binding was defined as [^{125}I]echistatin bound in the presence of an excess (1 μM final) of the cold unlabelled echistatin.

Competition binding studies were performed with a fixed concentration of [^{125}I]echistatin (0.05 and 0.1 nM for $\alpha_V\beta_3$ and $\alpha_V\beta_5$, respectively) and concentrations ranging from 200 μM to 1 nM of the tested peptides. All assays were performed in triplicate in a final volume of 0.2 mL, each containing the following species: 0.05 mL of [^{125}I]echistatin, 0.04 mL of tested peptide and 0.11 mL of blocking/binding buffer.

After incubation for 3 h at room temperature, the plate was washed three times with blocking/binding buffer, then 200 μL of MicroScint-40 liquid scintillation (PerkinElmer Life Sciences, Boston, MA) was added in each well and the plate was put into a Top-Count NXT microplate scintillation counter (PerkinElmer Life Sciences, Boston, MA) for the counting. Relativity affinity values (IC_{50}) were determined by fitting binding inhibition values by non-linear regression using GraphPad curve fitting software (PRISM, San Diego, CA). The reproducibility of the IC_{50} values was proved by performing the same tests on one of the antagonists reported by Belvisi et al.[9g]

5.2. Synthesis

5.2.1. General information. All the reactions requiring anhydrous conditions were carried out under nitrogen and the solvents were appropriately dried before use. Wang resin was purchased from Senn Chemicals (100–200 mesh, 1% DVB, 1.22 mmol/g) or from Calbiochem-Novabiochem AG (100–200 mesh, 1% DVB, 0.96 mmol/g). Peptide grade DMF was used for solid-phase peptide synthesis. NMR spectra were recorded with Varian Mercuryplus 400 spectrometer (H^1, 400 MHz). The NMR spectroscopic data are reported in δ (ppm) from TMS at 25 °C. Mass spectra were recorded with an Applied Biosystem ESI-TOF Mariner spectrometer by direct inlet. Polarimetric measures were performed on a JASCO DIP-370 polarimeter. Inter- and intramolecular coupling and Fmoc deprotection reactions were monitored using the Kaiser[25] and the bromophenol blue tests.[26]

5.2.2. *N*-Fmoc-Asp(Wang-resin)-OAll. DIC (0.20 mL, 1.26 mmol) was added to a solution of *N*-Fmoc-Asp-OAll (1.0 g, 2.53 mmol) in dry CH_2Cl_2 (8 mL) at 0 °C under nitrogen atmosphere. After stirring for 30 min, the solvent was removed under reduced pressure, the residue was dissolved in DMF (20 mL) and added with

DMAP (28 mg, 0.25 mmol). This solution was then added to the Wang resin (2.6 g, 0.96 mmol/g), preswollen in DMF for 30 min in a solid-phase reaction vessel. The reaction mixture was shaken for 1 h, then the solution was drained and the resin was washed with DMF (3× 20 mL) and CH_2Cl_2 (3× 20 mL), and dried. The resin loading (0.25 mmol/g) was determined through the Fmoc release monitored by UV absorption at 301 nm. The unreacted hydroxyl groups were capped by treatment with acetic anhydride (4.8 mL, 50.6 mmol) and NMM (5.6 mL, 50.6 mmol) in CH_2Cl_2 for 1.5 h. The resin was washed in sequence with CH_2Cl_2 (2× 20 mL), DMF (2× 20 mL) and CH_2Cl_2 (2× 20 mL) then dried under vacuum.

5.2.3. *N*-Fmoc-Gly-Asp-(Wang-resin)-OAll (3). The Fmoc protecting group was removed by treating twice the *N*-Fmoc-Asp(Wang-resin)-OAll resin (1.86 g, 0.25 mmol/g) with a 20% piperidine/DMF solution (18 mL, 1 × 10 min and 1 × 15 min) and then the resin was washed with DMF (5× 10 mL). The coupling was carried out by treating the resin with a mixture of *N*-Fmoc-Gly-OH (3 equiv, 415 mg), HOBt (3 equiv), TBTU (3 equiv) and NMM (6 equiv) in 18 mL DMF for 1.5 h. After the coupling the resin was washed with CH_2Cl_2 (3× 20 mL).

5.2.4. *N*-Fmoc-Arg(Pbf)-Gly-Asp-(Wang-resin)-OAll. The *N*-Fmoc-Gly-Asp-(Wang-resin)-OAll resin was deprotected with a *fast protocol* to avoid 2,5-diketopiperazine formation. In particular, the resin was treated with a 20% piperidine/DMF solution for an overall time of 15 min (18 mL, 3 × 5 min). The *N*-Fmoc-Arg(Pbf)-OH amino acid (3 equiv, 905 mg) was coupled following the same procedure described above for *N*-Fmoc-Gly-OH.

5.2.5. *N*-Fmoc-(2*R*,7a*R*)-GPTM-Arg(Pbf)-Gly-Asp-(Wang-resin)-OAll (4a). The Fmoc group was cleaved following the same deprotection procedure described above for the *N*-Fmoc-Asp(Wang-resin)-OAll resin. Then a suspension of HOBt (1.40 mmol), TBTU (1.40 mmol), NMM (2.79 mmol) and enantiopure *N*-Fmoc-(2*R*,7a*R*)-GPTM-OH (0.70 mmol) in DMF (8 mL) was added to H_2N-Arg(Pbf)-Gly-Asp-(Wang-resin)-OAll and the reaction mixture was shaken for 2 h. The resin was washed with CH_2Cl_2 (3× 20 mL).

5.2.6. *N*-Fmoc-(2*R*,7a*R*)-GPTM-Arg(Pbf)-Gly-Asp-(Wang-resin)-OH. The resin **4a** was swollen with dry CH_2Cl_2 (18 mL, 2 × 20 min) under argon atmosphere and shaken with a solution of $PhSiH_3$ (11.2 mmol) in dry CH_2Cl_2 (10 mL) for 5 min. A solution of $Pd(PPh_3)_4$ (0.14 mmol) in dry CH_2Cl_2 (5 mL) was then added and the resin was shaken for 45 min. The resin was washed with dry CH_2Cl_2 (20 mL, 1 × 5 min) and the procedure was repeated once again. Eventually, the resin was washed in sequence with CH_2Cl_2 (20 mL, 1 × 5 min), a 0.5% sodium diethyldithiocarbamate/DMF solution (20 mL, 3 × 5 min), DMF (20 mL, 3 × 2 min) and CH_2Cl_2 (20 mL, 3 × 2 min). The completeness of the deprotection was verified by performing a micro-cleavage on a few resin beads with a 5% H_2O/TFA solution and recording an ESI-MS spectrum of the product [735 (MH^+)].

5.2.7. Cyclo[(2*R*,7a*R*)-GPTM-Arg(Pbf)-Gly-Asp-(Wang-resin)]. The *N*-Fmoc-(2*R*,7a*R*)-GPTM-Arg(Pbf)-Gly-Asp-(Wang-resin)-OH resin was treated twice with a 20% piperidine/DMF solution (18 mL, 2 × 15 min) to remove the Fmoc group. The resin was washed with DMF (5× 10 mL). Then, a solution of TBTU (0.51 mmol) and DIPEA (0.93 mmol) in DMF (10 mL) was added to the supported linear pentapeptide and the mixture was shaken overnight. As usual (see general information), the completeness of the coupling was assessed using the Kaiser and bromophenol blue tests.

5.2.8. Cyclo[Arg-Gly-Asp-(2R,7aR)-GPTM] (5). The supported cyclic peptide cyclo[(2*R*,7a*R*)-GPTM-Arg(Pbf)-Gly-Asp-(Wang-resin)] was treated with a mixture of TFA/H_2O (95:5, 10 mL) for 2.5 h. The resin was filtered off and washed several times with CH_2Cl_2. The combined filtrates were concentrated under reduced pressure, precipitated from cold Et_2O, centrifuged and lyophilized to afford the crude product which was purified by flash chromatography on silica gel [CH_2Cl_2: MeOH (1% TFA) = 10:1 → 2:1] or by RP HPLC [Hypercarb 100 × 10 mm, 7 μm; t_R = 10 min, from 5% to 50% of B in 22 min; A = H_2O (0.1% formic acid), B = CH_3CN (0.1% formic acid)]. After lyophilization, the cyclic peptide **5** was obtained as a white powder. The purity of the sample was determined by RP HPLC [NUCLEODUR 100 C18 125 × 4.6 mm, 5 μm; t_R = 10 min, from 0% to 15% of B in 10 min; A = H_2O (0.1% TFA), B = CH_3CN (0.1% TFA) and Hypercarb 150 × 4.6 mm, 3 μm; t_R = 15 min, from 5% to 20% of B in 20 min; A = H_2O (0.1% formic acid, 3% CH_3CN), B = CH_3CN (0.1% formic acid, 3% H_2O)] and was greater than 95% as judged by the peak area at 214 nm. **5**: 21% overall yield (with respect to *N*-Fmoc-Asp(Wang-resin)-OAll loading); t_R = 6 min [Hypercarb 100 × 10 mm, 7 μm; from 5% to 50% of B in 22 min; A = H_2O (0.1% formic acid), B = CH_3CN (0.1% formic acid)]. MS (ESI): 495 (MH^+). $[\alpha]_D^{22}$ +88.7 (*c* 0.3, H_2O); ^1H NMR (400 MHz, D_2O) δ 4.37–4.26 (m, 2H; H–C_αArg, H–C_αAsp), 3.51 (dt, J = 11.6, 8.5 Hz, 1H; 5-H_aGPTM), 3.31–3.24 (m, 1H; 5-H_bGPTM), 3.17–3.07 (m, 2H; H–C_δArg), 2.96–2.91 (m, 1H; H–C_βAsp), 2.82–2.70 (m, 2H; H–C_βAsp, 1-H_aGPTM), 2.43 (dd, J = 14.8, 8.2 Hz, 1H; 1-H_bGPTM), 2.35 (dd, J = 12.2, 6.7 Hz, 1H; 7-H_aGPTM), 2.15–2.05 (m, 1H; 6-H_aGPTM), 1.97–1.77 (m, 2H; 6-H_bGPTM, H–C_βArg), 1.74–1.72 (m, 1H; H–C_βArg), 1.68–1.49 (m, 2H; 7-H_bGPTM, H–C_γArg), 1.22 (qd, J = 6.2, 1.0 Hz, 1H; H–C_γArg); ^{13}C NMR (100 MHz, D_2O) δ 175.9, 175.7, 174.1, 173.9, 172.8, 170.7 (s; CO), 156.6 (s; CN), 72.6 (s; C-7a GPTM), 57.9 (d; C-2 GPTM), 57.8 (d; C_α Arg), 53.7 (d; C_αAsp), 48.8 (t; C_αAly), 43.5 (t; C-5 GPTM), 40.3 (t; C_δArg), 39.4 (t; C-1 GPTM), 35.4 (t; C_βAsp), 33.9 (t; C-7 GPTM), 27.7 (t; C_βArg), 24.6 (t; C-6 GPTM), 24.4 (t; C_γArg); MS (ESI): 495 (MH^+).

5.2.9. Cyclo[Arg-Gly-Asp-(2*S*,7a*S*)-GPTM] (6). The synthesis was performed with the same procedure described above for diasteromer **5**, starting from enantiopure

(2*S*,7a*S*)-Fmoc-GPTM-OH (0.68 mmol) and *N*-Fmoc-Asp(Wang-resin)-OAll (1.6 g, 0.35 mmol/g loading). **6**: 14% overall yield (with respect to *N*-Fmoc-Asp(Wang-resin)-OAll loading). $t_R = 8$ min [Hypercarb 100 × 10 mm, 7 μm; from 5% to 50% of B in 22 min; A = H_2O (0.1% formic acid), B = CH_3CN (0.1% formic acid)]. MS (ESI): 495 (MH^+). $[\alpha]_D^{20}$ −44.0 (*c* 0.3, H_2O); ^1H NMR (400 MHz, D_2O) δ 4.10 (t, $J = 7.7$ Hz, 1H; H–C_αArg), 4.05 (d, $J = 14.2$ Hz, 1H; H–C_αGly), 3.42 (d, $J = 14.1$ Hz, 1H; H–C_αGly), 3.34 (dt, $J = 11.7$, 8.2 Hz, 1H; 5-H_aGPTM), 3.16–3.02 (m, 3H; 5-H_bGPTM, H–C_δArg), 2.78 (dd, $J = 7.6$, 6.0 Hz, 2H; H–C_βAsp), 2.47 (dd, $J = 14.3$, 8.2 Hz, 1H; 1-H_aGPTM), 2.29 (dd, $J = 12.3$, 5.7 Hz, 1H; 7-H_aGPTM), 2.13 (d, $J = 14.3$ Hz, 1H; 1-H_bGPTM), 2.12–2.08 (m, 1H; 6-H_aGPTM), 1.84–1.77 (m, 1H; 7-H_bGPTM), 1.70 (q, $J = 7.7$ Hz, 2H; H–C_βArg), 1.62–1.43 (m, 3H; 6-H_bGPTM, H–C_γArg); ^1H NMR (400 MHz, DMSO-d_6) δ 12.20 (br s, 1H; CO_2H), 8.66 (br t, $J = 6.1$ Hz, 1H; NH Gly), 8.41 (d, $J = 6.8$ Hz, 1H; NH Arg), 8.28 (d, $J = 9.0$ Hz, 1H; NH GPTM), 7.44 (br s, 2H; NH_2Arg), 7.40–7.38 (m, 1H; C═NH Arg), 7.13 (d, $J = 9.2$ Hz, 1H; NH Asp), 4.56 (dt, $J = 8.4$, 5.1 Hz, 1H; 2-H GPTM), 4.47 (dt, $J = 8.5$, 4.3 Hz, 1H; H–C_αAsp), 4.07 (q, $J = 7.2$ Hz, 1H; H–C_αArg), 4.00 (dd, $J = 13.9$, 7.8 Hz, 1H; H–C_αGly), 3.48–3.45 (m, 1H; 5-H_aGPTM), 3.19 (dd, $J = 13.9$, 4.4 Hz, 1H; H–C_αGly), 3.12–3.07 (m, 2H; H–C_δArg), 2.99–2.92 (m, 1H; 5-H_bGPTM), 2.69 (dd, $J = 16.7$, 8.4 Hz, 1H; 1-H_aGPTM), 2.41 (dd, $J = 16.7$, 4.8 Hz, 1H; 1-H_bGPTM), 2.34–2.29 (m, 3H; 7-H_aGPTM, H–C_βAsp), 2.09 (d, $J = 14.0$ Hz, 1H; 7-H_bGPTM), 1.85–1.77 (m, 1H; 6-H_aGPTM), 1.73–1.42 (m, 5H; 6-H_bGPTM, H–C_βArg, H–C_γArg); ^{13}C NMR (100 MHz, D_2O) δ 179.8, 177.41, 177.36, 174.4, 173.7, 173.5 (s; CO), 159.3 (s; CN), 77.3 (s; C-7a GPTM), 58.9 (d; C-2 GPTM), 57.7 (d; C_αArg), 51.6 (d; C_αAsp), 46.5 (t; C_αAly), 43.5 (t; C-5 GPTM), 43.0 (t; C_δArg), 41.7 (t; C-1 GPTM), 37.1 (t; C_βAsp), 36.8 (t; C-7 GPTM), 28.7 (t; C_βArg), 28.5 (t; C_γArg), 27.0 (t; C-6 GPTM); MS (ESI): 495 (MH^+).

Acknowledgments

The authors thank the Ministry of Instruction, University and Research (MiUR, Italy) for financial support (projects PRIN 2002031849 and 2004031072). Mrs. B. Innocenti is acknowledged for technical support.

References and notes

1. For recent reviews see: (a) Plow, E. F.; Haas, T. A.; Zhang, L.; Loftus, J.; Smith, J. W. *J. Biol. Chem* **2000**, *275*, 21785; (b) Humphries, M. J. *Biochem. Soc. Trans.* **2000**, *28*, 311; (c) Arnaout, M. A.; Goodman, S. L.; Xiong, J. P. *Curr. Opin. Cell Biol* **2002**, *14*, 641; (d) Hynes, R. O. *Cell* **2002**, *110*, 673; (e) Humphries, J. D.; Byron, A.; Humphries, M. J. *J. Cell Sci.* **2006**, *119*, 3901; (f) Luo, B.-H.; Carman, C. V.; Springer, T. A. *Annu. Rev. Immunol.* **2007**, *25*, 619.
2. Ruoslathi, E.; Pierschbacher, M. D. *Science* **1987**, *238*, 491.
3. (a) Eliceiri, B. P.; Cheresh, D. *Cancer J.* **2000**, *13*, 245; (b) Burke, P. A.; De Nardo, S. J.; Miers, L. A.; Lamborn, K. L.; Matzku, S.; De Nardo, G. L. *Cancer Res.* **2002**, *62*, 4263; (c) Haubner, R.; Finsinger, D.; Kessler, H. *Angew. Chem., Int. Ed.* **1997**, *36*, 1374; (d) Meyer, A.; Auernheimer, J.; Modlinger, A.; Kessler, H. *Curr. Pharm. Des.* **2006**, *12*, 2723; (e) Stupp, R.; Ruegg, C. *J. Clin. Oncol.* **2007**, *25*, 1637; (f) Hsu, A. R.; Veeravagu, A.; Cai, W.; Hou, L. C.; Tse, V.; Chen, X. *Recent Pat. Anti-Cancer Drug Discovery* **2007**, *2*, 143.
4. (a) Marinelli, L.; Gottschalk, K. E.; Meyer, A.; Novellino, E.; Kessler, H. *J. Med. Chem.* **2004**, *47*, 4166; (b) Friedlander, M.; Theesfeld, C. L.; Sugita, M.; Fruttiger, M.; Thomas, M. A.; Chang, S.; Cheresh, D. A. *Proc. Natl. Acad. Sci. U.S.A.* **1996**, *93*, 9764; (c) Friedlander, M.; Brooks, P. C.; Shaffer, R. W.; Kincaid, C. M.; Varner, J. A.; Cheresh, D. A. *Science* **1995**, *270*, 1500.
5. (a) Brooks, P. C.; Stromblad, S.; Klemke, R.; Visscher, D.; Sarkar, F. H.; Cheresh, D. A. *J. Clin. Invest.* **1995**, *96*, 1815; (b) Kumar, C. C.; Malkowski, M.; Yin, Z.; Tanghetti, E.; Yaremko, B.; Nechuta, T.; Varner, J.; Liu, M.; Smith, E. M.; Neustadt, B.; Presta, M.; Armstrong, L. *Cancer Res.* **2001**, *61*, 2232.
6. Mitjans, F.; Meyer, T.; Fittschen, C.; Goodman, S.; Jonczyk, A.; Marshall, J. F.; Reyes, G.; Piulats, J. *Int. J. Cancer* **2000**, *87*, 716.
7. MacDonald, T. J.; Taga, T.; Shimada, H.; Tabrizi, P.; Zlokovic, B. V.; Cheresh, D. A.; Laug, W. E. *Neurosurgery* **2001**, *48*, 151.
8. (a) Haubner, R.; Gratias, R.; Diefenbach, B.; Goodman, S. L.; Jonczyk, A.; Kessler, H. *J. Am. Chem. Soc.* **1996**, *118*, 7461; (b) Zimmermann, D.; Guthöhrlein, E. W.; Malešević, M.; Sewald, K.; Wobbe, L.; Heggemann, C.; Sewald, N. *Chem. Biol. Chem.* **2005**, *6*, 272; (c) Weide, T.; Modlinger, A.; Kessler, H. *Top. Curr. Chem.* **2007**, *272*, 1.
9. (a) Bach, A. C., Jr.; Espina, J. R.; Jackson, S. A.; Stouten, P. F. W.; Duke, J. L.; Mousa, S. A.; DeGrado, W. F. *J. Am. Chem. Soc.* **1996**, *118*, 293; (b) Dechantsreiter, M.; Planker, E.; Mathä, B.; Lohof, E.; Hölzemann, G.; Jonczyk, A.; Goodman, S. L.; Kessler, H. *J. Med. Chem.* **1999**, *42*, 3033; (c) Lohof, E.; Planker, E.; Mang, C.; Burkhart, F.; Dechantsreiter, M. A.; Haubner, R.; Wester, H. J.; Schwaiger, M.; Hölzemann, G.; Goodman, S. L.; Kessler, H. *Angew. Chem., Int. Ed.* **2000**, *39*, 2761; (d) Belvisi, L.; Bernardi, A.; Checchia, A.; Manzoni, L.; Potenza, D.; Scolastico, C.; Castorina, M.; Capelli, A.; Giannini, G.; Carminati, P.; Pisano, C. *Org. Lett.* **2001**, *3*, 1001; (e) Schumann, F.; Müller, A.; Sewald, N. *J. Am. Chem. Soc.* **2000**, *122*, 12009; (f) Casiraghi, G.; Rassu, G.; Auzzas, L.; Bureddu, P.; Gaetani, E.; Battistini, L.; Zanardi, F.; Curti, C.; Nicastro, G.; Belvisi, L.; Motto, I.; Castorina, M.; Giannini, G.; Pisano, C. *J. Med. Chem.* **2005**, *48*, 7675; (g) Belvisi, L.; Bernardi, A.; Colombo, M.; Manzoni, L.; Potenza, D.; Scolastico, C.; Giannini, G.; Marcellini, M.; Riccioni, T.; Castorina, M.; LoGiudice, P.; Carminati, P.; Pisano, C. *Bioorg. Med. Chem.* **2006**, *14*, 169; (h) Creighton, C. J.; Du, Y.; Santulli, R. J.; Tounge, B. A.; Reiz, A. B. *Bioorg. Med. Chem. Lett.* **2006**, *16*, 3971; (i) Urman, S.; Gaus, K.; Yang, Y.; Strijowski, U.; Sewald, N.; De Pol, S.; Reiser, O. *Angew. Chem., Int. Ed.* **2007**, *46*, 3976.
10. Tucker, G. C. *Curr. Oncol. Rep.* **2006**, *8*, 96.
11. (a) Pitts, W. J.; Wityak, J.; Smallheer, J. M.; Tobin, A. E.; Jetter, J. W.; Buynitsky, J. S.; Harlow, P. P.; Solomon, K. A.; Corjay, M. H.; Mousa, S. A.; Wexler, R. R.; Jadhav, P. K. *J. Med. Chem.* **2000**, *43*, 27; (b) Batt, D. G.; Petraitis, J.; Houghton, G. C.; Modi, D. P.; Cain, G. A.; Corjay, M. H.; Mousa, S. A.; Bouchard, P. J.; Forsythe, M. S.; Harlow, P. P.; Barbera, F. A.; Spitz, S. M.; Wexler, R. R.; Jadhav, P. K. *J. Med. Chem.* **2000**, *43*, 41.

12. (a) Pisaneschi, F.; Gensini, M.; Salvati, M.; Cordero, F. M.; Brandi, A. *Heterocycles* **2006**, *67*, 413; (b) Salvati, M.; Cordero, F. M.; Pisaneschi, F.; Bucelli, F.; Brandi, A. *Tetrahedron* **2005**, *61*, 8836; (c) Cordero, F. M.; Pisaneschi, F.; Salvati, M.; Valenza, S.; Faggi, C.; Brandi, A. *Chirality* **2005**, *17*, 149; (d) Cordero, F. M.; Pisaneschi, F.; Meschini Batista, K.; Valenza, S.; Machetti, F.; Brandi, A. *J. Org. Chem.* **2005**, *70*, 856; (e) Cordero, F. M.; Valenza, S.; Machetti, F.; Brandi, A. *Chem. Commun.* **2001**, 1590.
13. For a recent review on azabicyclic dipeptide mimetics, see: Maison, W.; Prenzel, A. H. G. P. *Synthesis* **2005**, 1031.
14. For a preliminary communication see: Salvati, M.; Cordero, F. M.; Pisaneschi, F.; Cini, N.; Bottoncetti, A.; Brandi, A. *Synlett* **2006**, *13*, 2067.
15. For recent reviews see: (a) Davies, J. S. *J. Pept. Sci.* **2003**, *9*, 471; (b) Lambert, J. N.; Mitchell, P.; Roberts, K. D. *J. Chem. Soc., Perkin Trans. 1* **2001**, *5*, 471; (c) Romanovskis, P.; Spatola, A. F. *J. Pept. Res.* **1998**, *52*, 356.
16. (a) Wang, P.; Miranda, L. P. *Int. J. Pept. Res. Ther.* **2005**, *11*, 117; (b) Alcaro, M. C.; Sabatino, G.; Uziel, J.; Chelli, M.; Ginanneschi, M.; Rovero, P.; Papini, A. M. *J. Peptide Sci.* **2004**, *10*, 218; (c) Teixido, M.; Altamura, M.; Quartara, L.; Giolitti, A.; Maggi, C. A.; Giralt, E.; Albericio, F. *J. Comb. Chem.* **2003**, *5*, 760; (d) McCusker, C. F.; Kocienski, P. J.; Boyle, F. T.; Schätzlein, A. G. *Bioorg. Med. Chem.* **2002**, *12*, 547; (e) Akaij, K.; Teruya, K.; Akaij, M.; Aimoto, S. *Tetrahedron* **2001**, *57*, 2293; (f) Kates, S. A.; Daniels, S. B.; Albericio, F. *Anal. Biochem.* **1993**, *212*, 303.
17. Kumar, C. C.; Nie, H.; Rogers, C. P.; Malkowski, M.; Maxwell, E.; Catino, J. J.; Armstrong, L. *J. Pharm. Exp. Ther.* **1997**, *283*, 843.
18. The use of [^{125}I]echistatin as competing ligand in receptor binding assays has been reported in previous literature, showing data consistent with our results (Refs. 5b,9g,17). However, binding affinity and selectivity could differ significantly when different competing ligands or different kind of binding assays and receptors are used. For example, **2** is reported to be 10-fold more selective for $\alpha_V\beta_3$ when vitronectin is used as the ligand in competition binding assay. See: Goodman, S. L.; Hölzemann, G.; Sulyok, G. A. G.; Kessler, H. *J. Med. Chem.* **2002**, *45*, 1045.
19. The proline residues in (*R*,*R*)-GPTM and (*S*,*S*)-GPTM are homofacial with L-(*S*)-proline and D-(*R*)-proline, respectively, but the configurational descriptors of the corresponding C-7a$_{GPTM}$ and Cα_{Pro} are opposite, because in GPTM the additional C-2 methylene has priority over the C-7 methylene group.
20. Xiong, J. P.; Stehle, T.; Zhang, R.; Joachimiak, A.; Frech, M.; Goodman, S. L.; Arnout, M. A. *Science* **2002**, *296*, 151.
21. For recent examples see: (a) Moitessier, N.; Henry, C.; Maigret, B.; Chapleur, Y. *J. Med. Chem.* **2004**, *47*, 4178; (b) Marinelli, L.; Lavecchia, A.; Gottschalk, K. E.; Novellino, E.; Kessler, H. *J. Med. Chem.* **2003**, *46*, 4393.
22. *F* is the ratio between the variance of the average distances and the average variances of the molecule distances.
23. The two ligands **5** and **6** are soluble in water, methanol and DMSO.
24. ACCELRYS, San Diego, CA.
25. Kaiser, E.; Colescott, R. L.; Bossinger, C. D.; Cook, P. I. *Anal. Biochem.* **1970**, *34*, 595.
26. Krchnak, V.; Vagner, J.; Safar, P.; Lebl, M. *Collect. Czech. Chem. Commun.* **1988**, *53*, 2542.